Cell Metabolism
Article

White to Brown Fat Phenotypic Switch Induced by Genetic and Environmental Activation of a Hypothalamic-Adipocyte Axis

Lei Cao,[1,2,3,*] Eugene Y. Choi,[1,2,3] Xianglan Liu,[1,2,3] Adam Martin,[1,2,3] Chuansong Wang,[1,2,3] Xiaohua Xu,[4] and Matthew J. During[1,2,3,*]
[1]Department of Molecular Virology, Immunology, and Medical Genetics
[2]Department of Neuroscience
[3]The Comprehensive Cancer Center
[4]Divison of Environmental Health Sciences, College of Public Health
The Ohio State University, Columbus, OH 43210, USA
*Correspondence: lei.cao@osumc.edu (L.C.), during.1@osu.edu (M.J.D.)
DOI 10.1016/j.cmet.2011.06.020

SUMMARY

Living in an enriched environment with complex physical and social stimulation leads to improved cognitive and metabolic health. In white fat, enrichment induced the upregulation of the brown fat cell fate determining gene Prdm16, brown fat-specific markers, and genes involved in thermogenesis and β-adrenergic signaling. Moreover, pockets of cells with prototypical brown fat morphology and high UCP1 levels were observed in the white fat of enriched mice associated with resistance to diet-induced obesity. Hypothalamic overexpression of BDNF reproduced the enrichment-associated activation of the brown fat gene program and lean phenotype. Inhibition of BDNF signaling by genetic knockout or dominant-negative trkB reversed this phenotype. Our genetic and pharmacologic data suggest a mechanism whereby induction of hypothalamic BDNF expression in response to environmental stimuli leads to selective sympathoneural modulation of white fat to induce "browning" and increased energy dissipation.

INTRODUCTION

Obesity and metabolic syndrome are rapidly becoming major global health, social, and economic problems with substantial morbidity and mortality (Batsis et al., 2007) highlighting the urgent need for new therapeutic strategies. Obesity results from chronic excess energy intake over energy expenditure and is controlled by variable and complicated interactions between genetic background, environmental factors, behavioral factors, and socioeconomic status. We sought to use environmental approaches to identify potential molecular therapeutic candidates and regulation pathways. Previously, we demonstrated that an enriched environment (EE), consisting of physically and socially more complex housing, leads to improved cerebral health as defined by increased neurogenesis, enhanced learning and memory, and resistance to external cerebral insults (Cao et al., 2004; Young et al., 1999). Moreover, we observed that the mice living in EE housing were leaner than those living in standard laboratory housing although they were fed ad libitum on identical diets. To further characterize this phenotype, we examined the molecular and morphological features of the fat. Two types of adipose tissue have been found in mammals, white adipose tissue (WAT) and brown adipose tissue (BAT). WAT and BAT are different at functional, morphological, and molecular levels. BAT dissipates energy directly as heat through uncoupling fatty acid oxidation from ATP production by uncoupling protein-1 (UCP1), is vital for the regulation of body temperature (Enerback et al., 1997), and is also involved in the control of body weight (Feldmann et al., 2009). BAT has recently become a potential target for pharmacological and genetic manipulation to treat human obesity because positron emission tomography has provided evidence that adult humans retain metabolically active BAT depots which can be induced in response to cold and sympathetic nervous system (SNS) activation (Cypess et al., 2009; van Marken Lichtenbelt et al., 2009; Virtanen et al., 2009). WAT accumulates excess energy as triacylglycerols and was previously viewed as a passive organ with relatively simple functions such as energy storage, heat insulation, and mechanical cushioning. However, recent developments have demonstrated that WAT is a versatile and more complex organ with many functions other than energy balance and that WAT is highly adaptive to external stimuli. Of interest, brown adipocyte-like cells are found in WAT of rodents and humans. These cells, with a multilocular morphology and expressing the brown adipocyte-specific UCP-1, are called brown-in-white (brite) cells, beige cells, or adaptive or recruitable brown adipocytes (Enerback, 2009; Petrovic et al., 2010). Although the precise origin of these cells is not fully defined, the development of these thermogenic-competent cells in WAT is greatly enhanced in response to chronic cold exposure or prolonged β-adrenergic stimulation (Cousin et al., 1992; Guerra et al., 1998; Himms-Hagen et al., 1994), and the occurrence of these cells is associated with resistance to obesity and metabolic diseases (Cederberg et al., 2001; Guerra et al., 1998; Leonardsson et al., 2004). Here we observed a white to brown fat transformation in

WAT of enriched mice associated with resistance to diet-induced obesity (DIO). Furthermore, we sought to identify the key components of the hypothalamic-adipocyte axis regulating this "browning" effect by pharmacological and genetic approaches.

RESULTS

EE Decreases Adiposity

C57BL/6 mice were randomly assigned to live in either grouped control housing or EE with larger space, running wheels, and regularly changed toys and mazes under an ambient temperature of 22°C. Both control and EE animals had free access to normal chow diet (NCD) and water. After 4 weeks EE, the EE mice had slightly lower body weights than control mice and a marked reduction in WAT mass (Figure 1A). All of the WAT pad weights were markedly decreased: inguinal WAT (IWAT) by 46.3% ± 4.8%, epididymal WAT (EWAT) by 46.7% ± 3.7%, and retroperitoneal WAT (RWAT) by 73.7% ± 2.5%. Magnetic resonance imaging (MRI) showed 49.3% ± 12.8% decrease of abdominal fat mass (Figure 1B). Since physical exercise decreases body fat, we subjected another group of mice to voluntary wheel running for 4 weeks. Running decreased body weight similarly to EE mice (Figure 1A). However, the reduction in WAT in runners was significantly less than that observed with EE (Figure 1A, $p < 0.05$). Both EE and running increased gastrocnemius mass, by 22.7% ± 3.5% and 12.8% ± 2.5%, respectively. We traced the traveling distance of EE mice plus the wheel running distance excluding activity within the feeding cage (the regular mouse cage) (Cao et al., 2010). The total distance traveled by the EE mice was 0.86 km/d more than control mice but approximately 66% lower than runner's average traveling distance 2 km/d/mouse, indicating the further reduction of adiposity was not due to greater overall motor activity in EE.

We measured the whole-body metabolism of mice after 5 weeks EE using the CLAMS for 3 days at room temperature. No difference in oxygen consumption was found in the EE mice compared to the control mice. However, the EE mice, upon removal from their complex environment, showed significantly lower physical activity in the metabolic chambers (see Figure S1A available online, $p < 0.05$). The change of environment from EE to single housing in the metabolic chamber and the impact on metabolism resulting from the coping behavior complicates the evaluation of energy expenditure. Therefore the data from the CLAMS may not properly represent the energy expenditure in the EE. In contrast to EE, wheel-running mice showed higher physical activity in the metabolic chambers compared to control mice, yet no significant increase in oxygen consumption was observed (Figures S1A and S1B), further demonstrating the limitation of CLAMS in the setting of acute environmental changes. We then used an alternative approach to measure metabolism for 3 hr starting immediately upon removal from the EE cage; the EE mice showed increased basal resting oxygen consumption at thermoneutrality (Figure 1D) (Feldmann et al., 2009). To supplement the whole body metabolism measurement, we measured the oxygen consumption of dissected fat depots ex vivo. The EE mice showed increased oxygen consumption in RWAT, whereas running mice showed higher oxygen consumption in BAT (Figure 1E). In addition, the EE mice showed increased food intake (Figure 1C), indicating that elevated energy expenditure rather than appetite suppression underlies the lean phenotype.

To further investigate the extent to which physical activity accounts for the lean phenotype induced by EE, we analyzed another group of mice housed in the EE cage with the running wheel removed. In addition, instead of being housed in the running wheel cages equipped to measure running distance in the previous experiment, the voluntary running group in this experiment was housed in the regular control cages with access to the same wheels as the EE mice. We monitored body weight closely over 9 weeks. In contrast to the 4 weeks EE with minimal handling, the runners were the only group that showed a significant decrease in body weight, while the body weight of EE mice with no access to running wheels was identical to that of the control mice (Figure 1F). However, the standard EE mice showed the most marked reduction in adiposity, with EWAT, RWAT, and IWAT decreased by 58.4% ± 3.6%, 70.0% ± 2.5%, and 46.5% ± 3.6%, respectively (Figure 1G). The EE no wheel mice showed a trend toward greater IWAT and EWAT mass reduction than the wheel running mice when fat mass was standardized to body weight (Figure 1G), suggesting that wheel running was not essential for the EE-induced fat mass reduction.

In order to investigate the potential mechanisms differentiating EE- and running-induced lean phenotypes, we profiled gene expression in the hypothalamus, one of the brain regions involved in energy homeostasis. EE and running led to multiple changes in the expression of genes involved in energy balance but displayed two distinctive profiles in the whole hypothalamus dissections after 4 weeks EE or running (Figure S1B). The hypothalamus contains a number of discrete nuclei including the arcuate (ARC), paraventricular (PVH), ventromedial (VMH), dorsomedial (DMH), and lateral hypothalamic area (LH). We previously observed differential gene expression profiles in the ARC, which has traditionally been considered a primary site for the central action of leptin on energy homeostasis (Stephens et al., 1995), of the EE mice compared to the running mice after 4 weeks of respective housing (Cao et al., 2010). Here we analyzed gene expression in the PVH, which was recently shown to be not simply downstream of the ARC but an additional primary site for a multinodal leptin/MC4R system regulating energy homeostasis (Ghamari-Langroudi et al., 2011). After 10 weeks EE or running, we observed two qualitatively distinct patterns in the PVH (Figure 1H). Running led to the induction of corticotrophin-releasing hormone (CRH) accompanied by the significant downregulation of its two receptors, Crhr1 and Crhr2. EE showed a trend of upregulation of thyrotropin-releasing hormone (TRH) in contrast to the trend of downregulation in the running mice (Figure 1H), suggesting that the EE and running reduce adiposity via distinct mechanisms. Thyroid hormones increase energy expenditure via a process termed "thyroid thermogenesis" (Cannon and Nedergaard, 2010), and recent findings suggest thyroid hormones affect the hypothalamus and subsequently activate BAT, leading to increased energy expenditure (Lopez et al., 2010). EE upregulated Trh expression in the hypothalamus; however, hyperthyroidism was not observed in mice after 9 weeks EE (serum T3, control 0.746 ± 0.025 ng/ml, EE 0.649 ± 0.036 ng/ml, $p = 0.062$; T4, control 4.52 ± 0.18 μg/dl, EE 3.15 ± 0.38 μg/dl, $p = 0.01$;

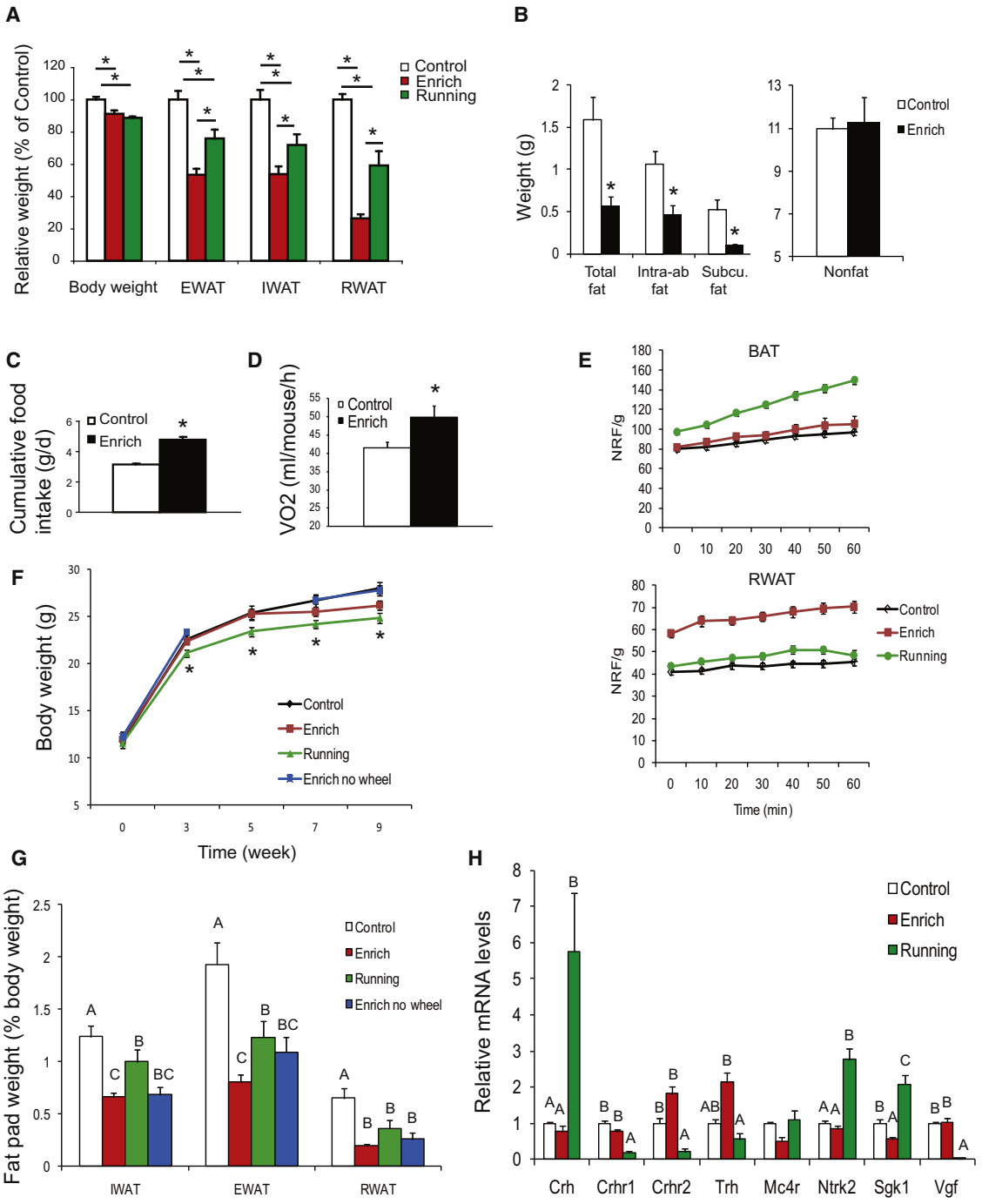

Figure 1. EE Decreases Adiposity of Mice Fed on NCD

(A) Four weeks of EE or wheel running decreased body weight and fat pad mass (n = 10 per group).

(B) MRI analysis of abdominal fat and lean mass (n = 5 per group). Intra-ab., intra-abdominal; Subcu., subcutaneous.

(C) EE increased food intake (n = 10 per group).

(D) EE increased basal resting oxygen consumption (n = 8 per group); *p < 0.05.

(E) EE increased oxygen consumption in RWAT ex vivo (p < 0.05 EE compared to control and running, n = 3 per group). Running increased oxygen consumption in BAT (p < 0.05 running compared to control and EE, n = 3 per group). NRF, normalized relative fluorescence.

(F) EE and EE no wheel did not decrease body weight, whereas wheel running decreased body weight (n = 10–20 per group) *p < 0.05 for running.

(G) Fat pad mass calibrated to body weight (n = 10–19 per group).

(H) Gene expression profile of the PVH after 10 weeks respective housing (n = 5 per group). Bars not connected by same letter are significantly different. Data are means ± SEM. See also Figure S1.

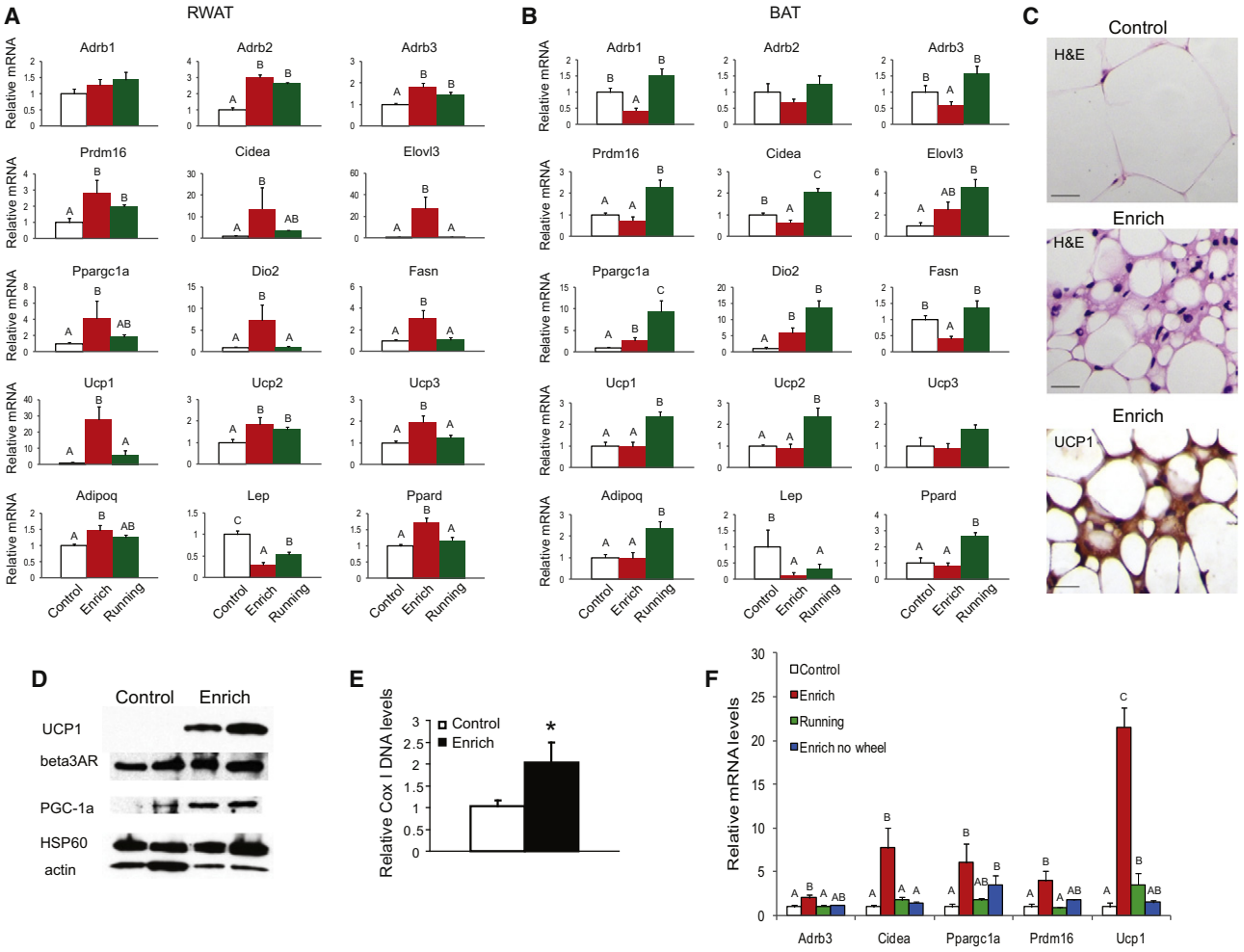

Figure 2. EE Induces Brown Fat Molecular Features in White Fat

(A and B) Gene expression profile of RWAT (A) and BAT (B) after 4 weeks of respective housing (n = 5 per group).

(C) H&E staining and UCP1 immunohistochemistry of RWAT. Scale bar, 20 μm.

(D) Western blot of RWAT.

(E) Mitochondrial DNA content of RWAT (n = 4 per group); *p < 0.05.

(F) Gene expression profile of RWAT after 9 weeks of respective housing (n = 4 per group). Bars not connected by the same letter are significantly different. Data are means ± SEM. See also Figure S2.

TSH, control 0.112 ± 0.024 μg/ml, EE 0.095 ± 0.024 μg/ml, p = 0.64).

EE Induces Brown Fat Molecular Phenotype in WAT

BAT and WAT perform opposing functions, with WAT accumulating surplus energy while BAT dissipates energy as heat. We examined the impact of EE on BAT and WAT gene expression profiles by quantitative RT-PCR after 4 weeks of EE (Figures 2A and 2B, Figures S2A and S2B). Limited gene expression changes were observed in BAT, with 6 out of the 19 genes profiled showing significant change (Figure 2B, Figure S2B). In contrast, RWAT was far more responsive to the EE, with 15 out of the 19 genes profiled showing altered expression (Figure 2A, Figure S2A). *Prdm16* (PR-domain-containing 16), which has been identified as a genetic switch determining the formation and function of brown adipocytes (Seale et al., 2008) was significantly upregulated by 2.8- ± 0.8-fold in RWAT. The induction of *Prdm16* was accompanied by the robust induction of a BAT molecular signature including *Cidea* (13.6- ± 1.0-fold), *Elovl3* (27.4- ± 11.2-fold), *Ucp1* and *Ppargc1a* (encoding PGC-1α), all of which are BAT-selective markers and positively regulated by *Prdm16* (Seale et al., 2008). PGC-1α has been shown to switch cells from energy storage to energy expenditure phenotype by inducing mitochondrial biogenesis and genes involved in thermogenesis (Puigserver et al., 1998). Data from knockout mouse strains suggest that several transcriptional regulators, such as RIP140 (Leonardsson et al., 2004), SRC2 (Picard et al., 2002), Rb (Hansen et al., 2004), and Twist1 (Pan et al., 2009), control brown adipocyte development and function, at least in part through regulating the transcriptional activity or gene expression of PGC-1α. This transcriptional coactivator was upregulated 4.1- ± 2.1-fold in RWAT of EE mice. BAT dissipates energy via

releasing chemical energy from mitochondria in the form of heat. This phenomenon is primarily mediated by UCP 1 (*Ucp1*), which is a specific BAT marker (Nicholls and Locke, 1984). *Ucp1* was increased 27.7- ± 8.0-fold in RWAT of EE mice. Other uncoupling proteins with a role in protection against oxidative damage, *Ucp2* and *Ucp3*, were also upregulated. In addition, *Dio2* (type 2 5′ deiodinase) and *Ppard*, both involved in oxidative metabolism, were upregulated by 7.3- ± 3.7-fold and 1.7- ± 0.1-fold, respectively. β-adrenergic signaling plays an important role in the activation of BAT in response to cold and the regulation of adiposity (Bachman et al., 2002; Himms-Hagen et al., 1994; Xue et al., 2007). Both *Adrb2* and *Adrb3* encoding β-adrenergic receptor (AR) 2 and 3 were upregulated in RWAT of EE mice (Figure 2A), while *Adrb1* and *Adrb3* were downregulated in BAT (Figure 2B). In contrast to the strong induction of the brown adipocyte gene program in RWAT, EE suppressed the expression of the white fat-enriched gene *Resn* (resistin) and had no impact on adipocyte markers shared by both brown and white fat such as adipogenic transcription factor *Pparg* and adipocyte differentiation marker *Ap2* (Kajimura et al., 2008) (Figure S2A). H&E staining showed that the RWAT adipocytes of EE mice were smaller than those in the control mice (Figure 2C). No increase in apoptosis measured by TUNEL was observed in EE mice (Figure S2C). Moreover, pockets of cells with the multilocular morphology characteristic of brown adipocytes (Tsukiyama-Kohara et al., 2001) were observed in RWAT (Figure 2C). Immunohistochemical staining showed substantially higher levels of UCP1 protein not only in the cells with typical brown fat morphology but also in some cells with unilocular white fat morphology surrounding the pocket of brown fat-like cells (Figure 2C) (Tsukiyama-Kohara et al., 2001). Western blot showed marked increase of UCP1, mitochondrial protein HSP60, β3AR, and PGC-1α levels in RWAT of EE mice (Figure 2D), consistent with the upregulation of mRNAs. Moreover, the mitochondrial DNA content of EE RWAT was increased by 2-fold, indicating enhanced mitochondrial biogenesis (Figure 2E) (Xue et al., 2007). The other two white fat pads, EWAT (Figure S2D) and IWAT (Figure S2E), showed fewer genetic changes compared to RWAT. However, expression of the major adipokine, leptin (*Lep*), was highly suppressed in all fat pads (Figures 2A and 2B, Figures S2D and S2E), consistent with the observed sharp drop in leptin serum levels (64.3% ± 4.0% decrease).

Although efficient in reducing adiposity, voluntary wheel running for 4 weeks induced different gene expression profiles in BAT and RWAT compared to EE. Running led to more robust changes in BAT than EE (Figure 2B). However, less BAT-selective genes were induced in RWAT of the running mice (Figure 2A). We analyzed the RWAT gene expression profiles after 10 weeks EE, wheel running, and EE without wheel. The standard EE induced the most robust BAT gene program in RWAT, while the effects of wheel running and EE without wheel were not additive (Figure 2F). The molecular signatures in fat induced by the different environmental interventions suggest distinctive molecular mechanisms underlying the reduction in adiposity in response to EE and running.

EE Inhibits DIO

EE induced a "browning" molecular signature in white fat suggesting that an individual's interaction with its immediate environment could switch a white fat energy storage phenotype to a brown fat-like energy expenditure phenotype and regulate adiposity. To test this hypothesis, we investigated whether this transformation could help animals resist DIO. The chow was changed to a high-fat diet (HFD, 45% fat, caloric density 4.73 kcal/g) immediately after mice were randomly assigned to live in EE or control housing. After 4 weeks HFD feeding, the EE mice gained less weight (71.3% ± 2.7% of control mice weight gain, Figures 3A and 3D) and remained lean with significantly smaller fat pads ($p < 0.01$, Figures 3B, 3C, and 3E). No change in food intake was observed (Figure 3F). The body temperature of EE mice was increased (EE, 34.86°C ± 0.20°C versus control, 34.17°C ± 0.14°C, $p = 0.01$), suggesting that elevated energy expenditure, not appetite suppression, led to the resistance to obesity. Moreover, EE prevented DIO associated hyperinsulinemia, hyperleptinemia, hyperglycemia, and dyslipidemia (Figure 3G). Similar to NCD, EE also induced the BAT molecular signature in DIO mice (Figure 3H), and the levels of *Ppargc1a* and *Prdm16* were inversely correlated with RWAT mass (Figures 3I and 3J, $p < 0.0001$), consistent with a robust functional effect of these molecular changes.

Long-Term EE Leads to Stronger WAT "Browning"

EE of 4 weeks was sufficient to induce WAT "browning" and resistance to DIO. We then investigated the long-term effect of EE for 3 months. In EE mice fed on NCD, clear macroscopic changes in fat pads were visible to the eye, with WAT turning brown and BAT going even darker (Figure 4A). Brown adipocyte-like cells were found in EWAT of long-term EE mice (Figure 4B), which was rare in short-term EE mice. The expressions of brown fat gene markers were further upregulated in EWAT (Figure 4C, Figure S2D). In contrast to pockets of brown adipocyte-like cells with UCP1 expression found in RWAT of short-term EE mice, widespread and stronger staining of UCP1 was observed in long-term EE mice (Figure 4D) associated with more robust induction of the brown fat gene program (Figure 4E). For example, *Elovl3* was upregulated by 118- ± 53.4-fold after 3 months EE, while it was induced by 27.4- ± 11.2-fold after 4 weeks EE. Despite their different anatomy and function, brown and white adipocytes are found together in fat depots, and the WAT/BAT ratio varies with genetic background, sex, age, nutritional status, and environmental conditions supporting the concept of an adipose organ, a multidepot organ consisting of two tissues displaying considerable plasticity (Frontini and Cinti, 2010). The darker BAT depot observed in long-term EE may indicate a shift toward brown adipocytes in this depot and/or enhanced thermogenic activity that requires further investigation.

EE Enhances WAT Response to Sympathetic Stimulation

The thermogenic activity of BAT is dependent on intact sympathetic stimulation (Landsberg and Young, 1984), and SNS stimulation is essential to induce brown fat-like cells in WAT depots (Cannon and Nedergaard, 2004). BAT is profusely innervated by sympathetic nerve terminals with norepinepherine (NE) acting via β-ARs. WAT is also innervated, although to a lesser degree (Slavin and Ballard, 1978; Youngstrom and Bartness, 1995). In mice fed on a NCD, EE led to an approximate 2-fold increase of NE in WAT (EE 50.0 ± 6.2 pg/mg versus control

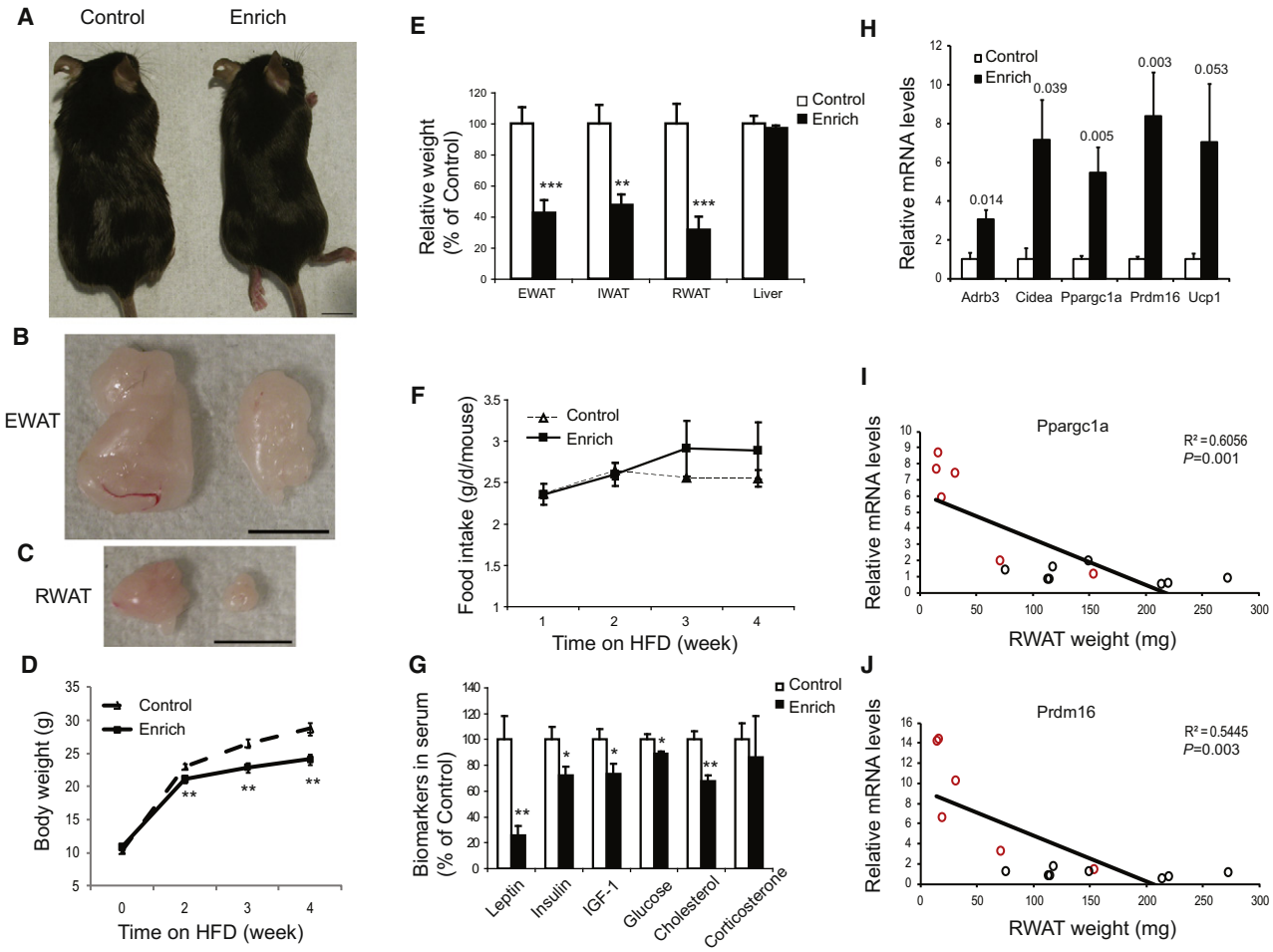

Figure 3. EE Prevents DIO

(A–C) EE mice remained lean compared to control mice when fed on HFD. Scale bar, 1 cm.

(D and E) EE mice had less weight gain (D) and fat mass (E) (n = 10 per group).

(F) Food intake.

(G) Biomarkers in serum.

(H) Gene expression profile in RWAT (n = 5 per group). P values of significance were shown above the bars.

(I and J) *Ppargc1a* and *Prdm16* mRNA levels were inversely correlated to RWAT weight. Red circles, individual EE mouse; black circles, individual control mouse.

*p < 0.05, **p < 0.01, ***p < 0.001. Data are means ± SEM.

25.1 ± 3.8 pg/mg, p = 0.012) while no significant increase was observed in serum, muscle, or BAT. Although NE content per se is not an index of NE release or sympathetic tone, the coordinated upregulation of β-ARs and NE levels in WAT is consistent with a change in β-AR signaling and might partially explain the selective regulation of WAT by EE.

Given the fact that EE led to a marked reduction of adiposity, we sought to investigate whether this reduction would influence the animals' response to cold. Mice of 3 months EE or control housing were randomized to be maintained at 4°C or 22°C. After 3 hr acute cold exposure, the EE mice maintained a similar body temperature as control mice (Figure S3A). We examined the expression of genes involved in thermogenesis and known to be activated in response to cold in both BAT and WAT. Both *Dio2* and *Ppargc1a* expression levels were higher in BAT of EE mice than control mice at 22°C, and their expression was upregulated after cold exposure (Figure S3B). Both genes were also upregulated in response to cold in control mice BAT (Figure S3B). However, in RWAT of control mice, neither *Dio2* nor *Ppargc1a* was changed after cold exposure, consistent with the lack of role for WAT in acute cold response (Figure S3B). In contrast, *Dio2* expression in RWAT of EE mice was 5.43- ± 1.47-fold higher than control mice at 22°C, and its expression levels were further upregulated by another 2.55- ± 0.22-fold in response to cold (Figure S3B), suggesting an enhanced molecular response of the EE WAT to acute cold. We further examined the sensitivity of RWAT of EE mice to NE stimulation at thermoneutrality of 30°C. Mice of 10 weeks EE were injected with NE (0.3 mg/kg, s.c.) under anesthesia, and the expression of genes known to be regulated by NE (Petrovic et al., 2010) was examined in RWAT 4 hr after NE injection. The low-dose NE failed to induce significant changes in control RWAT (Figure 4F). In

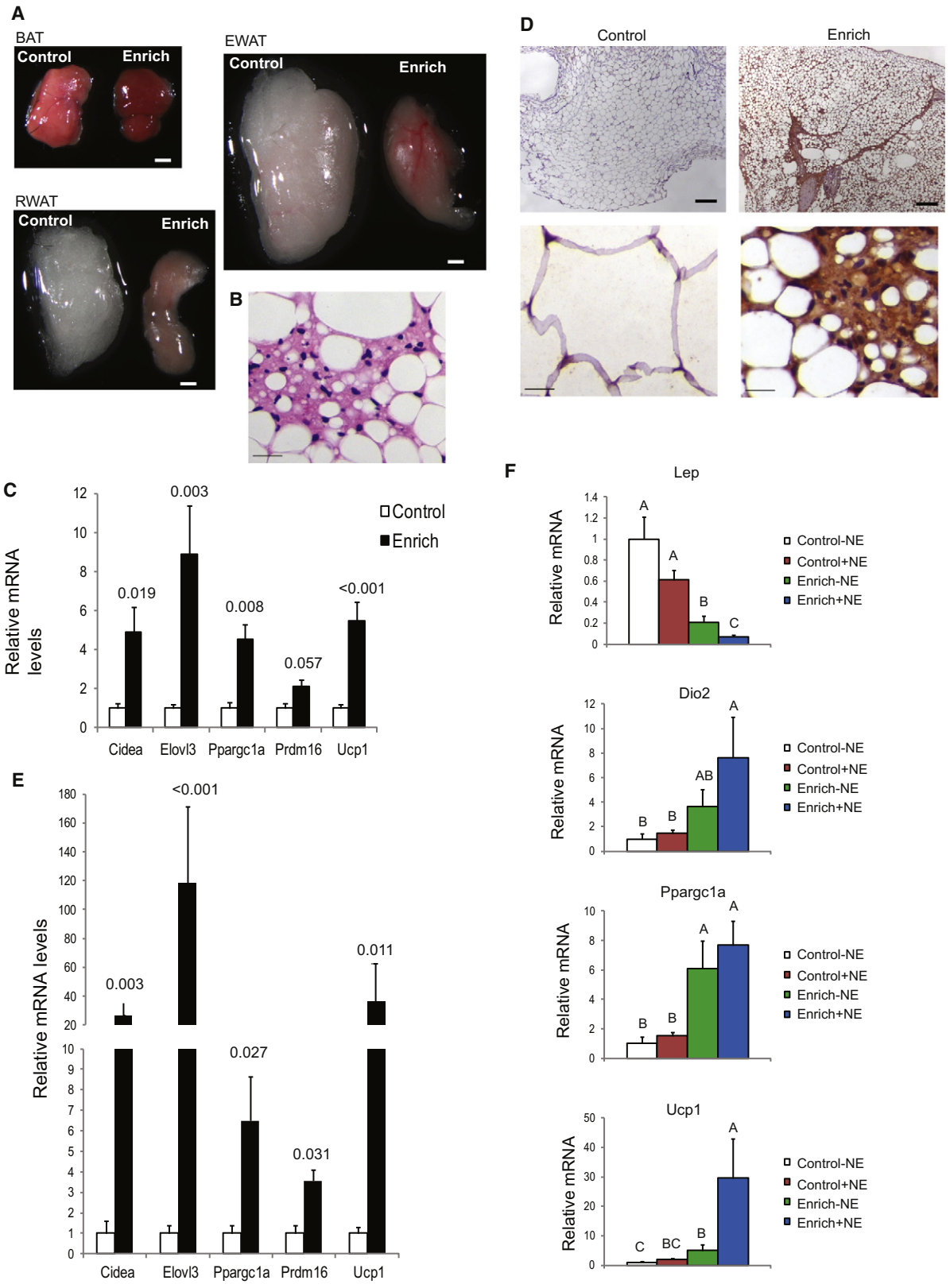

Figure 4. Long-Term EE Leads to Stronger White Fat "Browning"

(A) Representatives of BAT, EWAT, and RWAT of control or EE mice after 3 months EE. Scale bar, 1 mm.

(B) H&E staining of EWAT. Scale bar, 20 μm.

contrast, RWAT of EE mice was highly responsive to acute low-dose NE stimulation. *Lep* which was sharply downregulated in EE RWAT compared to control mice was further reduced significantly after NE injection. *Ucp1* was highly increased by NE stimulation in the EE RWAT (Figure 4F).

We then investigated the role of the global sympathetic drive in mediating EE regulation of WAT by using the β-blocker propranolol. Mice receiving propranolol in their drinking water were randomly assigned to live in EE or control housing for 5 weeks. Propranolol efficiently blocked the molecular features associated with EE (Figure S3C), suggesting the essential involvement of the SNS.

Hypothalamic-Adipocyte Axis Mediates EE-Induced WAT "Browning"

We recently report that EE inhibits tumor growth. The anticancer effect is mediated by hypothalamic brain-derived neurotrophic factor (BDNF) via activation of the hypothalamic-sympathoneural-adipocyte (HSA) axis (Cao et al., 2010). Using laser capture microdissection, we found a consistent upregulation in hypothalamic BDNF in EE mice but not in voluntary running (Cao et al., 2010). BDNF has recently been identified as a key element in energy homeostasis (Lyons et al., 1999; Rios et al., 2001; Xu et al., 2003). Our previous studies have demonstrated that hypothalamic gene transfer of BDNF leads to marked weight loss and alleviation of obesity and diabetes (Cao et al., 2009). Here we further investigated the role of BDNF in EE-induced "browning" of WAT. A rAAV vector expressing the human BDNF gene was injected to the hypothalamus of DIO mice with YFP as a control (Cao et al., 2009). The transgene expression level, location (ARC and VMH), and duration were similar to the previous studies (Cao et al., 2009, 2010). BDNF overexpression led to marked weight loss and fat depletion (Figures 5A–5C, Figure S4A), which reproduced the impact of EE on DIO mice but to a greater degree (Figure 3E). Similarly, BDNF overexpression resulted in the EE-associated molecular features, e.g., upregulation of β-ARs and BAT markers in RWAT (Figure 5D). Consistent with the marked increase in proteins involved in thermogenesis and mitochondrial function, e.g., UCP1 and HSP60 (Figure 5E, Figure S4B), all dissected fat depots of BDNF mice showed substantially higher oxygen consumption ex vivo (Figure S4C). The BDNF-overexpressing mice showed similar gene expression changes to EE mice in the whole hypothalamus dissections (Figure S4D). We further investigated whether β-blockade could attenuate hypothalamic BDNF's regulation of WAT. AAV-BDNF or empty viral vectors were injected to the hypothalamus bilaterally. Eight weeks after viral vector injection when both the change in body weight (BDNF, −3.8 ± 0.8 g versus empty vector, +2.9 ± 0.6 g, $p < 0.001$) and cumulative food intake (BDNF, 4.77 ± 0.13 g/d versus empty vector, 4.04 ± 0.18 g/d, $p = 0.004$) had stabilized, mice were randomly assigned to receive the combination of the β1 β2 blocker propranolol (2 mg/kg/d for 14 days) and β3 blocker SR59230A (1 mg/kg/d for 14 days) or vehicle delivered by osmotic minipumps. The β blockade efficiently attenuated the hypothalamic BDNF-induced gene program in WAT (Figure S4E).

To further define the role of BDNF, we evaluated several strategies including the use of BDNF heterozygous mice ($BDNF^{+/-}$) that develop adult-onset obesity associated with hypothalamic BDNF protein levels approximately 40% lower than wild-type (Lyons et al., 1999). We observed a substantial increase in the fat pad mass of $BDNF^{+/-}$ mice before a significant body weight difference occurred (Figure 6A). The molecular features of RWAT in $BDNF^{+/-}$ mice were a complete reversal of that found with EE or BDNF-overexpressing mice, namely a suppression of β-ARs and BAT gene program (Figure 6B). However, altered expression of β-ARs was not observed in muscles of either $BDNF^{+/-}$ mice (Figure S5A) or EE mice (Figure S5B), suggesting a selective modulation of fat β-AR signaling. We then used a dominant-negative truncated form of the high-affinity BDNF receptor (TrkB.T1) to specifically inhibit BDNF signaling in the hypothalamus of adult mice. Mice receiving rAAV-TrkB.T1 consumed more food (Figure S5C) and gained more weight than AAV-YFP controls (Figure S5D). Hypothalamic expression of TrkB.T1 reversed the gene expression changes associated with BDNF overexpression in the hypothalamus (Figures S5E and S4D), suggesting efficient inhibition of BDNF signaling. Similar to DIO mice, RWAT was enlarged in TrkB.T1 mice associated with the obesity. The molecular signature of RWAT was similar to $BDNF^{+/-}$ mice (Figure 6B). In order to examine whether the observed changes in RWAT were simply a result of obesity, we compared the RWAT molecular features between the DIO model receiving YFP control virus and TrkB.T1-induced obesity model. Although both models were identically obese (Figure 6C), TrkB.T1 led to a further increase of *Lep* expression above that of the DIO model (Figure 6D). Thus both global and hypothalamic-specific inhibition of BDNF led to a complete reversal of the EE-associated molecular features in WAT, indicating BDNF's involvement in WAT gene program regulation. Furthermore, we investigated whether BDNF mediated the EE-associated molecular "browning" of WAT by using microRNA to block EE-induced BDNF upregulation in hypothalamus (Cao et al., 2009). We generated AAV vectors expressing a microRNA targeting Bdnf (miR-Bdnf) and a microRNA targeting a scrambled sequence (miR-scr.) (Cao et al., 2010). We injected rAAV vectors of miR-Bdnf or miR-scr. into the hypothalamus and then assigned the mice to standard or EE housing for 4 weeks. MicroRNA knockdown of BDNF led to accelerated weight gain by approximately 2-fold. In mice receiving miR-scr., the EE-induced molecular signatures of RWAT were maintained (Figure 6E). In contrast, miR-Bdnf efficiently inhibited EE-induced hypothalamic BDNF upregulation (Cao et al., 2010) and completely blocked the molecular changes in WAT associated with EE (Figure 6E).

(C) Gene expression profile of EWAT (n = 4 per group).
(D) Immunohistochemical staining of UCP1 in RWAT. Scale bar, 200 μm in the upper panels, 20 μm in the lower panels.
(E) Gene expression profile of RWAT (n = 4 per group). *P* values are shown above the bars.
(F) Gene expression profile of RWAT 4 hr after NE injection (n = 4 per group). Bars not connected by the same letter are significantly different. Data are means ± SEM. See also Figure S3.

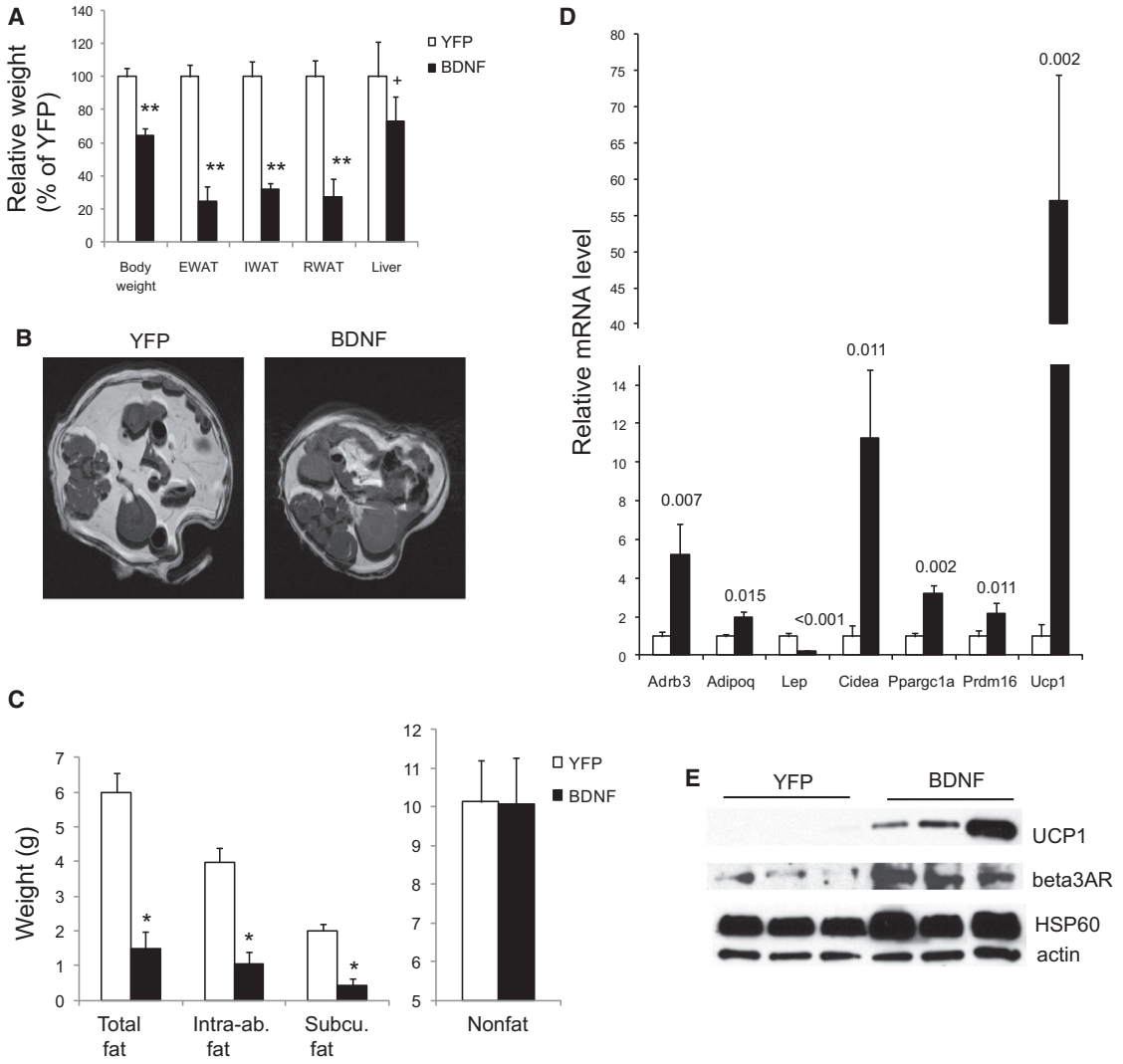

Figure 5. Hypothalamic BDNF Mediates EE-Induced WAT to BAT Transformation

(A) rAAV-mediated gene delivery of BDNF to hypothalamus reproduced EE-associated reduction of adiposity.

(B) Representative images of adipose tissues by MRI.

(C) MRI analysis of abdominal fat and lean mass (n = 4 per group) *p < 0.05. Intra-ab., intra-abdominal; Subcu., subcutaneous.

(D) Gene expression profile of RWAT of BDNF-overexpressing mice and YFP control mice. n = 4 BDNF, n = 5 YFP. P values are shown above the bars.

(E) Western blot of RWAT. Data are means ± SEM. See also Figure S4.

DISCUSSION

The development of obesity is influenced by the balance between BAT and WAT. The proneness to obesity in most rodent models reportedly correlates with decreased BAT activity, while the resistance to obesity correlates with increased BAT function or the emergence of brown adipocyte-like cells or gene expression in WAT (Chiang et al., 2009; Leonardsson et al., 2004; Pan et al., 2009; Seale et al., 2011; Tsukiyama-Kohara et al., 2001; Vegiopoulos et al., 2010). Recent studies demonstrate that adult humans have metabolically active BAT which can be activated in response to cold temperature with the presence of BAT correlating inversely with body fat (Nedergaard et al., 2007; Saito et al., 2009; van Marken Lichtenbelt et al., 2009; Virtanen et al., 2009; Zingaretti et al., 2009). Furthermore, several histological studies have reported brown adipocytes dispersed among white fat in 24% of adult humans biopsies and reaching 50% of cases with exclusion of patients over 50 years old (Nedergaard et al., 2007). In addition, studies of human fat cell dynamics show a high turnover rate of adipocytes with approximately 10% of fat cells being renewed annually at all adult ages and levels of body mass index (Spalding et al., 2008). Human white adipocytes from subcutaneous fat tissues can be manipulated in vitro to develop "brown" characteristics by forced expression of PGC-1α (Tiraby et al., 2003). These findings further suggest the therapeutic potential of BAT-oriented strategies to enhance energy expenditure by facilitating brown adipocyte maintenance and function, stimulating pre-existing brown precursors, and

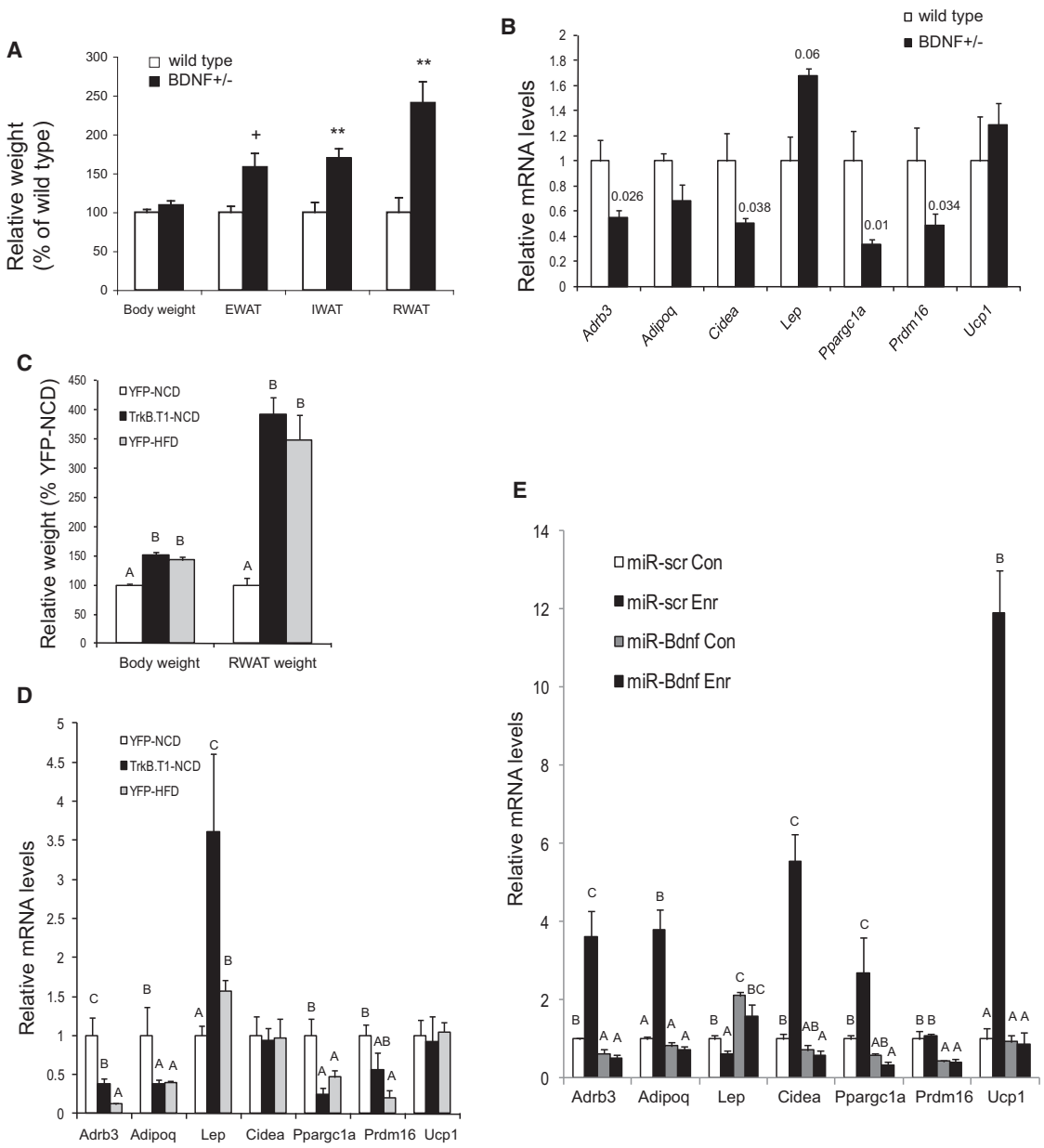

Figure 6. BDNF Inhibition Blocks the EE-Induced WAT to BAT Transformation

(A) Increase of adiposity occurred before weight increase in BDNF$^{+/-}$ mice compared to wild-type littermates. n = 4 per group. **p < 0.01, +p < 0.06.

(B) RWAT gene expression profile of BDNF$^{+/-}$ mice compared to wild-type litter mates (n = 4 per group). P values are shown above the bars.

(C) TrkB.T1-expressing mice were equally obese as DIO mice expressing YFP (n = 5 per group).

(D) RWAT gene expression profile of TrkB.T1-expressing mice compared to lean YFP control mice fed with NCD and obese YFP mice fed with HFD (n = 5 per group).

(E) MicroRNA targeting BDNF blocked EE-associated molecular features of RWAT (n = 4 per group; Con, control housing; Enr, EE housing). Bars not connected by the same letter are significantly different. Data are means ± SEM. See also Figure S5.

inducing the specific gene program to favor white-to-brown adipocyte transformation (Enerback, 2010; Frontini and Cinti, 2010; Kajimura et al., 2010). Our data demonstrate that EE induces a molecular and functional switch from WAT to BAT in the absence of chronic cold or prolonged pharmacological β-adrenergic stimulation.

The molecular characteristics of EE-induced WAT "browning" include induction of brown fat molecular switch Prdm16 and brown fat markers such as *Ucp1*, *Ppragc1a*, *Elovl3* and *Cidea*; suppression of white fat-enriched gene *Resn*; and no changes in adipocyte markers shared by both white and brown fat such as *Pparg* and *Ap2*. Recent studies have shown that

thiazolidinediones (TZDs), a family of insulin sensitizers and ligands for PPARγ, cause WAT browning, but the associated risk of cardiac and bone side effects and an increase in fat mass (Farmer, 2008) limit their potential in obesity treatment. In this context, EE shows advantages over TZDs because it selectively induces genes involved in mitochondrial biogenesis and oxygen consumption, thereby switching WAT to the BAT phenotype without affecting lipogenic genes or the threat of obesity associated with TZD treatment.

The emergence of brown adipocytes in WAT is under genetic control, with large differences among inbred strains of mice (Guerra et al., 1998). C57BL/6 mice, the strain we used in all of our experiments, respond poorly to sympathetic activation, probably due to low levels of β-AR expression (Guerra et al., 1998; Xue et al., 2007). Cold exposure at 5°C for 7 days or daily injection of a β3 agonist for 14 days failed to induce brown adipocytes in RWAT in C57BL/6 mice with only sporadic, low induction of *Ucp1* expression (Guerra et al., 1998). In contrast, EE led to a 27-fold induction of *Ucp1* in this strain (Figure 2A), which can be compared to the 9-fold induction observed in the same strain of mice acclimated to 5°C cold for 4 weeks or the 23-fold induction after daily injection of β agonist CL316243 for 11–12 days (Vegiopoulos et al., 2010). Of interest, EE significantly induced both β_2 and β_3 AR expression in RWAT (Figure 2A), suggesting the absence of the desensitization of β ARs after extended exposure to β agonists (Arner, 1992). In addition, an acute low-dose NE led to downregulation of *Lep* and upregulation of *Ucp1* only in the EE RWAT, suggesting the enhanced sensitivity to NE stimulation (Figure 4F). Further investigation is required to definitively clarify whether the increased sympathetic tone to the WAT or the increased β-AR levels in the WAT enhancing its sensitivity to the SNS activity, or both, are responsible for the induction of BAT program.

Adaptive thermogenesis, defined as the regulated production of heat in response to environmental temperature or diet, is involved in the development of obesity (Lowell and Spiegelman, 2000). Large interindividual differences in cold-induced (nonshivering) and diet-induced adaptive thermogenesis exist in animals and humans. Moreover, the individual metabolic responses to both cold exposure and overfeeding are related, suggesting a shared regulatory mechanism (Wijers et al., 2009). The regulatory mechanisms of cold exposure and sympathetic activation have been extensively investigated in rodents, which are thought to operate similarly in humans (Nedergaard et al., 2007). Here we observed a new type of adaptive thermogenesis in mice, EE-induced adaptive thermogenesis in response to a complex environment, which also requires SNS activation. The β-blocker propranolol administration sufficiently blocked the EE-induced gene program in WAT (Figure S3C). Although systemic β blockade affects various tissues, the efficient blockade of molecular signature in WAT at least suggests an intact β-AR signaling is required for the EE-induced browning. Selective denervation of each fat pad and electrophysiological or neurochemical measurement of SNS drive will further define the role of SNS in this EE-associated adaptive thermogenesis.

The original theories of SNS activation proposed a body-wide increase in sympathetic outflow (Cannon, 1929). More recent studies suggest that independent autonomic inputs to individual organs through distinct autonomic projections permit fine-tuning of metabolism (Anderson et al., 1987). Our data suggest a selective SNS regulation of WAT by EE with no significant effects on blood pressure or heart rate (Figure S3D). Studies using the retrograde neuronal tracer pseudorabies virus (PRV) reveal that the SNS has a distinct organization in different body compartments. Dual tracing of RWAT and IWAT finds no colocalization in PVH or amygdala (Kreier et al., 2006). In addition, there is differential SNS drive among WAT depots as well as between WAT and BAT after food deprivation, cold exposure, or glucoprivation (Brito et al., 2008). For example, RWAT NE turnover (NETO) increases with glucoprivation and cold, while BAT NETO is unaffected by glucoprivation or food deprivation. The mechanisms underlying this fat pad-specific pattern of SNS drive remain to be elucidated. We speculate that specific neurons in the PVH or other parts of the SNS output such as brain stem (Foster et al., 2010; Grill, 2010) may be activated by specific environmental stimulations or physiological conditions and regulate SNS drive in a fat depot-specific manner, and we are currently investigating the identity of these neurons in the EE mice.

EE consists of increased dynamic social interactions, frequent exposure to novel objects, and enhanced physical activity. It is unlikely that a single variable accounts for all the effects of EE. Indeed, several lines of evidence suggest exercise alone does not account for the EE-induced phenotype: (1) EE reduced adiposity more effectively than wheel running (Figures 1A and 1G), (2) EE showed less physical activity than wheel running, (3) EE no wheel was able to decrease adiposity (Figure 1G), (4) EE and wheel-running mice displayed different behavioral adaptation in CLAMS (Figure S1A), (5) EE showed increased oxygen consumption in RWAT whereas wheel running showed an increase in BAT (Figure 1E), (6) at the level of transcription, EE induced changes primarily in RWAT while wheel running influenced gene expression mainly in BAT (Figures 2A and 2B), and (7) EE and wheel running showed two qualitatively distinct gene expression profiles in PVH (Figure 1H) and whole hypothalamus (Figure S1B). However, the removal of running wheels attenuated WAT browning induced by EE, suggesting that access to wheels is an important part of the complex environment provided in EE (Figure 2F). In future studies, we plan to dissect out which components of EE (sensory, cognitive, motor, and social stimulation) are essential for WAT browning and how the brain appraises and responds to different environmental conditions leading to distinct peripheral changes. Here we propose one mechanism: the induction of hypothalamic BDNF expression in response to environmental stimuli leading to sympathoneural activation (Figure 7). Several lines of evidence support the role of BDNF: (1) EE induced BDNF expression in the hypothalamus together with immediate early genes such as *Fos* and *Junb*, markers of neuronal activity (Cao et al., 2010). The upregulation of BDNF expression observed as early as 2 weeks EE suggests that BDNF is involved early in the regulation of the activity of hypothalamus, a brain structure that integrates the hypothalamic pituitary axis and the SNS (Ulrich-Lai and Herman, 2009), monitors and regulates the energetic state of the body (Ruffin and Nicolaidis, 1999), and modulates the SNS outflow to both BAT and WAT (Foster et al., 2010; Perkins et al., 1981). (2) Hypothalamic overexpression of BDNF mimicked EE-induced "browning" of WAT (Figure 5D). (3) Inhibition of hypothalamic BDNF function by TrkB.T1 or

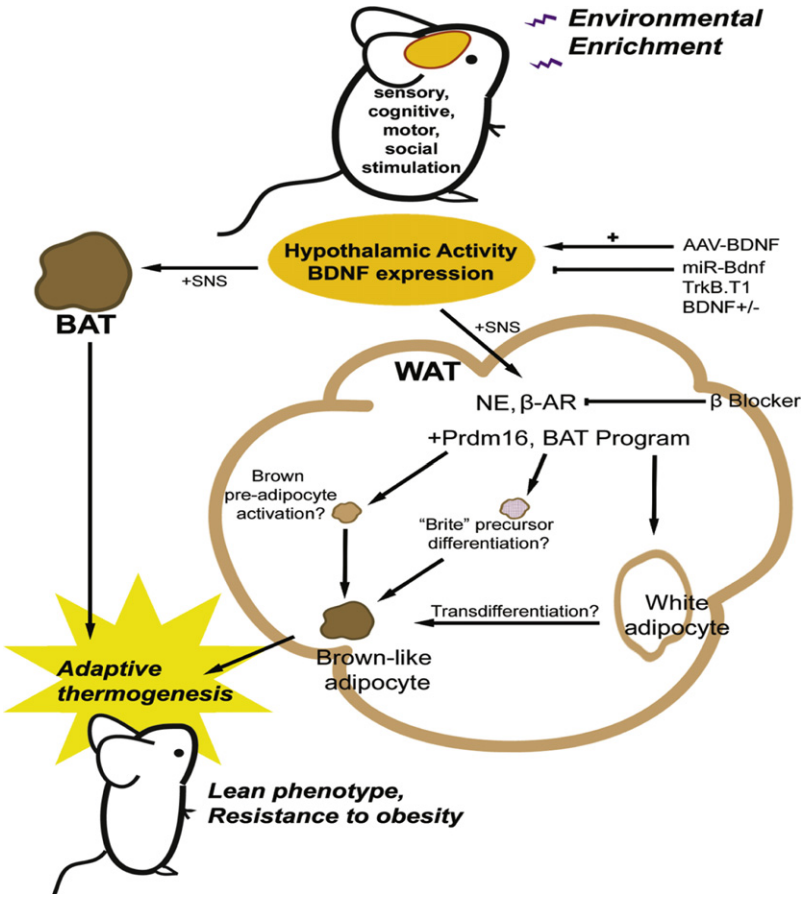

Figure 7. Mechanism of EE-Induced White Fat "Browning"
See the Discussion for details.

$BDNF^{+/-}$ mice led to a complete reversal of the EE-associated molecular features in WAT (Figures 6B and 6D). (4) Inhibition of the EE-induced BDNF upregulation in hypothalamus by microRNA blocked the EE-induced brown fat molecular signature (Figure 6E). (5) β-AR blockade attenuated EE- or hypothalamic BDNF overexpression-induced WAT browning (Figures S3C and S4E).

Our data suggest hypothalamic BDNF expression signals to increase SNS outflow to WAT. The downstream mediators and pathways of BDNF remain to be elucidated. BDNF receptor TrkB is expressed in the PVH, an area involved in the SNS outflow to WAT (Foster et al., 2010). Both CRH and TRH neurons in PVH express TrkB (Levin, 2007). Both EE and BDNF overexpression led to upregulation of *Crh* and *Trh* (Figures S1B and S4D). In contrast, inhibition of hypothalamic BDNF signaling by TrkB.T1 downregulated *Crh* and *Trh*. Both CRH and TRH have thermogenic property via the SNS and therefore could mediate the actions of BDNF (Levin, 2007). However, the upregulation of *Crh* was not sustained in PVH with 10 weeks of EE, while *Trh* maintained higher levels of expression (Figure 1H). Of interest, recent evidence suggests that thyroid hormones increase energy metabolism through a central effect on the hypothalamus and thereby regulate BAT activity (Cannon and Nedergaard, 2010; Lopez et al., 2010). No increase in serum T3, T4, or TSH was observed in the EE mice. However, the expression of type 2 deiodinase (D2) was induced in WAT by EE (Figure 2A). D2 activates the prohormone T4 and thereby increases the local availability of the biologically active T3, leading to production of extra heat (Leonard et al., 1983; Watanabe et al., 2006). Whether TRH is downstream of BDNF in this central pathway modulating fat remains to be determined.

The origin of the brown-like cells requires further investigation. Recent studies have shown that BAT and skeletal muscle originate from Myf5+ precursors with *Prdm16* controlling classical brown adipocyte fate (Seale et al., 2008), and transgenic expression of Prdm16 in fat tissue induces the brown-like cells in subcutaneous WAT but not intraabdominal WAT depots (Seale et al., 2011). Prdm16 was modestly but significantly upregulated in WAT of EE mice (Figure 2A), suggesting possible recruitment of prebrown adipocyte. However, at least two possibilities remain: white to brown transdifferentiation or the activation of "brite" (brown-in-white) adipocytes that are thermogenically competent but developmentally and molecularly distinct from classical brown adipocytes (Petrovic et al., 2010). The adaptive UCP1-expressing brown-like cells that emerge in WAT in response to cold or β-adrenergic stimulation are not descendent from the same cell lineage as the classical brown adipocyte but derived predominantly by white to brown adipocyte transdifferentiation (Barbatelli et al., 2010; Timmons et al., 2007). Further elucidation of the nature of the brown-like cells induced by EE and the pathways underlying this CNS regulation of fat phenotype could provide potential therapeutic strategies for obesity treatment.

In summary, our data demonstrate that EE decreases adiposity; increases energy expenditure; causes resistance to obesity; and induces a genetic, morphological, and functional transformation from WAT to BAT through a central mechanism with hypothalamic BDNF as the key mediator linking environmental stimuli, sympathetic outflow, and the "browning" of white fat and subsequent energy dissipation.

EXPERIMENTAL PROCEDURES

EE Protocol

Male 3-week-old C57Bl/6 mice were housed in EE cage as detailed in the Supplemental Experimental Procedures. We carried out all mice experiments in compliance with the regulations of the Institutional Animal Ethics Committees.

Voluntary Running Experiment

Male 3-week-old C57/BL6 mice were housed in cages with free access to running wheels (Med Associates) as detailed in the Supplemental Experimental Procedures.

EE with No Access to Running Wheel Experiment

We randomly assigned 3-week-old C57/BL6 mice to 4 groups: control housing, EE housing (as described above), EE with no access to running wheel (remove the wheel from EE cage), and wheel running in regular cage (a wheel placed in regular mouse cage). The mice were maintained in the respective housing conditions for 10 weeks.

EE Protocol with HFD

We randomly assigned 20 C57Bl/6 mice to live in EE or control housing as described above for 4 weeks. We switched the diet from NCD to HFD (45% fat, caloric density 4.73 kcal/g, Research Diets, Inc.) when EE was initiated.

AAV-Mediated BDNF Overexpression in DIO Mice

We randomly assigned DIO mice (approximately 40 g) to receive AAV-BDNF or AAV-YFP as detailed in the Supplemental Experimental Procedures. Mice were maintained on HFD throughout the experiment.

AAV-MicroRNA Experiment

We randomly assigned 7-week-old C57/BL6 mice to receive AAV-miR-Bdnf (n = 12) or AAV-miR-scr (n = 12) as detailed in the Supplemental Experimental Procedures. Ten days after surgery, half of the miR-Bdnf mice and miR-scr. mice were housed in EE housing with the other half of the groups maintained in standard housing. After 4 weeks of EE housing, we dissected fat pads and analyzed the gene expression using qRT-PCR.

Statistical Analysis

Data are expressed as mean ± SEM. We used JMP software to analyze the following: repeated-measures ANOVA for food intake and oxygen consumption; one-way ANOVA for serum biomarker measurements, body weight, and adipose tissue weight, body temperature, quantitative RT-PCR data; and regression for adipose tissue weight-gene expression correlation.

SUPPLEMENTAL INFORMATION

Supplemental Information includes five figures, Supplemental Experimental Procedures, and Supplemental References and can be found with this article online at doi:10.1016/j.cmet.2011.06.020.

ACKNOWLEDGMENTS

We thank Dr. Qinghua Sun for advice on MRI analysis of fat mass and blood pressure measurement. We are grateful to Dr. Naresh Bal for assistance with oxygen consumption assays and Dr. F. Lee of Weill Medical College of Cornell University for providing the $BDNF^{+/-}$ mice. This work was supported in part by the National Institutes of Health.

Received: December 8, 2010
Revised: May 7, 2011
Accepted: June 21, 2011
Published: September 6, 2011

REFERENCES

Anderson, E.A., Wallin, B.G., and Mark, A.L. (1987). Dissociation of sympathetic nerve activity in arm and leg muscle during mental stress. Hypertension *9*, III114–III119.

Arner, P. (1992). Adrenergic receptor function in fat cells. Am. J. Clin. Nutr. *55*, 228S–236S.

Bachman, E.S., Dhillon, H., Zhang, C.Y., Cinti, S., Bianco, A.C., Kobilka, B.K., and Lowell, B.B. (2002). betaAR signaling required for diet-induced thermogenesis and obesity resistance. Science *297*, 843–845.

Barbatelli, G., Murano, I., Madsen, L., Hao, Q., Jimenez, M., Kristiansen, K., Giacobino, J.P., De Matteis, R., and Cinti, S. (2010). The emergence of cold-induced brown adipocytes in mouse white fat depots is determined predominantly by white to brown adipocyte transdifferentiation. Am. J. Physiol. Endocrinol. Metab. *298*, E1244–E1253.

Batsis, J.A., Nieto-Martinez, R.E., and Lopez-Jimenez, F. (2007). Metabolic syndrome: from global epidemiology to individualized medicine. Clin. Pharmacol. Ther. *82*, 509–524.

Brito, N.A., Brito, M.N., and Bartness, T.J. (2008). Differential sympathetic drive to adipose tissues after food deprivation, cold exposure or glucoprivation. Am. J. Physiol. *294*, R1445–R1452.

Cannon, W.B. (1929). Organization for physiological homeostasis. Physiol. Rev. *9*, 399–431.

Cannon, B., and Nedergaard, J. (2004). Brown adipose tissue: function and physiological significance. Physiol. Rev. *84*, 277–359.

Cannon, B., and Nedergaard, J. (2010). Thyroid hormones: igniting brown fat via the brain. Nat. Med. *16*, 965–967.

Cao, L., Jiao, X., Zuzga, D.S., Liu, Y., Fong, D.M., Young, D., and During, M.J. (2004). VEGF links hippocampal activity with neurogenesis, learning and memory. Nat. Genet. *36*, 827–835.

Cao, L., Lin, E.J., Cahill, M.C., Wang, C., Liu, X., and During, M.J. (2009). Molecular therapy of obesity and diabetes by a physiological autoregulatory approach. Nat. Med. *15*, 447–454.

Cao, L., Liu, X., Lin, E.J., Wang, C., Choi, E.Y., Riban, V., Lin, B., and During, M.J. (2010). Environmental and genetic activation of a brain-adipocyte BDNF/leptin axis causes cancer remission and inhibition. Cell *142*, 52–64.

Cederberg, A., Gronning, L.M., Ahren, B., Tasken, K., Carlsson, P., and Enerback, S. (2001). FOXC2 is a winged helix gene that counteracts obesity, hypertriglyceridemia, and diet-induced insulin resistance. Cell *106*, 563–573.

Chiang, S.H., Bazuine, M., Lumeng, C.N., Geletka, L.M., Mowers, J., White, N.M., Ma, J.T., Zhou, J., Qi, N., Westcott, D., et al. (2009). The protein kinase IKKepsilon regulates energy balance in obese mice. Cell *138*, 961–975.

Cousin, B., Cinti, S., Morroni, M., Raimbault, S., Ricquier, D., Penicaud, L., and Casteilla, L. (1992). Occurrence of brown adipocytes in rat white adipose tissue: molecular and morphological characterization. J. Cell Sci. *103*, 931–942.

Cypess, A.M., Lehman, S., Williams, G., Tal, I., Rodman, D., Goldfine, A.B., Kuo, F.C., Palmer, E.L., Tseng, Y.H., Doria, A., et al. (2009). Identification and importance of brown adipose tissue in adult humans. N. Engl. J. Med. *360*, 1509–1517.

Enerback, S. (2009). The origins of brown adipose tissue. N. Engl. J. Med. *360*, 2021–2023.

Enerback, S. (2010). Human brown adipose tissue. Cell Metab. *11*, 248–252.

Enerback, S., Jacobsson, A., Simpson, E.M., Guerra, C., Yamashita, H., Harper, M.E., and Kozak, L.P. (1997). Mice lacking mitochondrial uncoupling protein are cold-sensitive but not obese. Nature *387*, 90–94.

Farmer, S.R. (2008). Molecular determinants of brown adipocyte formation and function. Genes Dev. *22*, 1269–1275.

Feldmann, H.M., Golozoubova, V., Cannon, B., and Nedergaard, J. (2009). UCP1 ablation induces obesity and abolishes diet-induced thermogenesis in mice exempt from thermal stress by living at thermoneutrality. Cell Metab. *9*, 203–209.

Foster, M.T., Song, C.K., and Bartness, T.J. (2010). Hypothalamic paraventricular nucleus lesion involvement in the sympathetic control of lipid mobilization. Obesity (Silver Spring) *18*, 682–689.

Frontini, A., and Cinti, S. (2010). Distribution and development of brown adipocytes in the murine and human adipose organ. Cell Metab. *11*, 253–256.

Ghamari-Langroudi, M., Srisai, D., and Cone, R.D. (2011). Multinodal regulation of the arcuate/paraventricular nucleus circuit by leptin. Proc. Natl. Acad. Sci. USA *108*, 355–360.

Grill, H.J. (2010). Leptin and the systems neuroscience of meal size control. Front. Neuroendocrinol. *31*, 61–78.

Guerra, C., Koza, R.A., Yamashita, H., Walsh, K., and Kozak, L.P. (1998). Emergence of brown adipocytes in white fat in mice is under genetic control. Effects on body weight and adiposity. J. Clin. Invest. *102*, 412–420.

Hansen, J.B., Jorgensen, C., Petersen, R.K., Hallenborg, P., De Matteis, R., Boye, H.A., Petrovic, N., Enerback, S., Nedergaard, J., Cinti, S., et al. (2004). Retinoblastoma protein functions as a molecular switch determining white versus brown adipocyte differentiation. Proc. Natl. Acad. Sci. USA *101*, 4112–4117.

Himms-Hagen, J., Cui, J., Danforth, E., Jr., Taatjes, D.J., Lang, S.S., Waters, B.L., and Claus, T.H. (1994). Effect of CL-316,243, a thermogenic beta 3-agonist, on energy balance and brown and white adipose tissues in rats. Am. J. Physiol. *266*, R1371–R1382.

Kajimura, S., Seale, P., Tomaru, T., Erdjument-Bromage, H., Cooper, M.P., Ruas, J.L., Chin, S., Tempst, P., Lazar, M.A., and Spiegelman, B.M. (2008). Regulation of the brown and white fat gene programs through a PRDM16/CtBP transcriptional complex. Genes Dev. *22*, 1397–1409.

Kajimura, S., Seale, P., and Spiegelman, B.M. (2010). Transcriptional control of brown fat development. Cell Metab. *11*, 257–262.

Kreier, F., Kap, Y.S., Mettenleiter, T.C., van Heijningen, C., van der Vliet, J., Kalsbeek, A., Sauerwein, H.P., Fliers, E., Romijn, J.A., and Buijs, R.M. (2006). Tracing from fat tissue, liver, and pancreas: a neuroanatomical framework for the role of the brain in type 2 diabetes. Endocrinology *147*, 1140–1147.

Landsberg, L., and Young, J.B. (1984). The role of the sympathoadrenal system in modulating energy expenditure. Clin. Endocrinol. Metab. *13*, 475–499.

Leonard, J.L., Mellen, S.A., and Larsen, P.R. (1983). Thyroxine 5′-deiodinase activity in brown adipose tissue. Endocrinology *112*, 1153–1155.

Leonardsson, G., Steel, J.H., Christian, M., Pocock, V., Milligan, S., Bell, J., So, P.W., Medina-Gomez, G., Vidal-Puig, A., White, R., et al. (2004). Nuclear receptor corepressor RIP140 regulates fat accumulation. Proc. Natl. Acad. Sci. USA *101*, 8437–8442.

Levin, B.E. (2007). Neurotrophism and energy homeostasis: perfect together. Am. J. Physiol. *293*, R988–R991.

Lopez, M., Varela, L., Vazquez, M.J., Rodriguez-Cuenca, S., Gonzalez, C.R., Velagapudi, V.R., Morgan, D.A., Schoenmakers, E., Agassandian, K., Lage, R., et al. (2010). Hypothalamic AMPK and fatty acid metabolism mediate thyroid regulation of energy balance. Nat. Med. *16*, 1001–1008.

Lowell, B.B., and Spiegelman, B.M. (2000). Towards a molecular understanding of adaptive thermogenesis. Nature *404*, 652–660.

Lyons, W.E., Mamounas, L.A., Ricaurte, G.A., Coppola, V., Reid, S.W., Bora, S.H., Wihler, C., Koliatsos, V.E., and Tessarollo, L. (1999). Brain-derived neurotrophic factor-deficient mice develop aggressiveness and hyperphagia in conjunction with brain serotonergic abnormalities. Proc. Natl. Acad. Sci. USA *96*, 15239–15244.

Nedergaard, J., Bengtsson, T., and Cannon, B. (2007). Unexpected evidence for active brown adipose tissue in adult humans. Am. J. Physiol. Endocrinol. Metab. *293*, E444–E452.

Nicholls, D.G., and Locke, R.M. (1984). Thermogenic mechanisms in brown fat. Physiol. Rev. *64*, 1–64.

Pan, D., Fujimoto, M., Lopes, A., and Wang, Y.X. (2009). Twist-1 is a PPARdelta-inducible, negative-feedback regulator of PGC-1alpha in brown fat metabolism. Cell *137*, 73–86.

Perkins, M.N., Rothwell, N.J., Stock, M.J., and Stone, T.W. (1981). Activation of brown adipose tissue thermogenesis by the ventromedial hypothalamus. Nature *289*, 401–402.

Petrovic, N., Walden, T.B., Shabalina, I.G., Timmons, J.A., Cannon, B., and Nedergaard, J. (2010). Chronic peroxisome proliferator-activated receptor gamma (PPARgamma) activation of epididymally derived white adipocyte cultures reveals a population of thermogenically competent, UCP1-containing adipocytes molecularly distinct from classic brown adipocytes. J. Biol. Chem. *285*, 7153–7164.

Picard, F., Gehin, M., Annicotte, J., Rocchi, S., Champy, M.F., O'Malley, B.W., Chambon, P., and Auwerx, J. (2002). SRC-1 and TIF2 control energy balance between white and brown adipose tissues. Cell *111*, 931–941.

Puigserver, P., Wu, Z., Park, C.W., Graves, R., Wright, M., and Spiegelman, B.M. (1998). A cold-inducible coactivator of nuclear receptors linked to adaptive thermogenesis. Cell *92*, 829–839.

Rios, M., Fan, G., Fekete, C., Kelly, J., Bates, B., Kuehn, R., Lechan, R.M., and Jaenisch, R. (2001). Conditional deletion of brain-derived neurotrophic factor in the postnatal brain leads to obesity and hyperactivity. Mol. Endocrinol. *15*, 1748–1757.

Ruffin, M., and Nicolaidis, S. (1999). Electrical stimulation of the ventromedial hypothalamus enhances both fat utilization and metabolic rate that precede and parallel the inhibition of feeding behavior. Brain Res. *846*, 23–29.

Saito, M., Okamatsu-Ogura, Y., Matsushita, M., Watanabe, K., Yoneshiro, T., Nio-Kobayashi, J., Iwanaga, T., Miyagawa, M., Kameya, T., Nakada, K., et al. (2009). High incidence of metabolically active brown adipose tissue in healthy adult humans: effects of cold exposure and adiposity. Diabetes *58*, 1526–1531.

Seale, P., Bjork, B., Yang, W., Kajimura, S., Chin, S., Kuang, S., Scime, A., Devarakonda, S., Conroe, H.M., Erdjument-Bromage, H., et al. (2008). PRDM16 controls a brown fat/skeletal muscle switch. Nature *454*, 961–967.

Seale, P., Conroe, H.M., Estall, J., Kajimura, S., Frontini, A., Ishibashi, J., Cohen, P., Cinti, S., and Spiegelman, B.M. (2011). Prdm16 determines the thermogenic program of subcutaneous white adipose tissue in mice. J. Clin. Invest. *121*, 96–105.

Slavin, B.G., and Ballard, K.W. (1978). Morphological studies on the adrenergic innervation of white adipose tissue. Anat. Rec. *191*, 377–389.

Spalding, K.L., Arner, E., Westermark, P.O., Bernard, S., Buchholz, B.A., Bergmann, O., Blomqvist, L., Hoffstedt, J., Naslund, E., Britton, T., et al. (2008). Dynamics of fat cell turnover in humans. Nature *453*, 783–787.

Stephens, T.W., Basinski, M., Bristow, P.K., Bue-Valleskey, J.M., Burgett, S.G., Craft, L., Hale, J., Hoffmann, J., Hsiung, H.M., Kriauciunas, A., et al. (1995). The role of neuropeptide Y in the antiobesity action of the obese gene product. Nature *377*, 530–532.

Timmons, J.A., Wennmalm, K., Larsson, O., Walden, T.B., Lassmann, T., Petrovic, N., Hamilton, D.L., Gimeno, R.E., Wahlestedt, C., Baar, K., et al. (2007). Myogenic gene expression signature establishes that brown and white adipocytes originate from distinct cell lineages. Proc. Natl. Acad. Sci. USA *104*, 4401–4406.

Tiraby, C., Tavernier, G., Lefort, C., Larrouy, D., Bouillaud, F., Ricquier, D., and Langin, D. (2003). Acquirement of brown fat cell features by human white adipocytes. J. Biol. Chem. *278*, 33370–33376.

Tsukiyama-Kohara, K., Poulin, F., Kohara, M., DeMaria, C.T., Cheng, A., Wu, Z., Gingras, A.C., Katsume, A., Elchebly, M., Spiegelman, B.M., et al. (2001). Adipose tissue reduction in mice lacking the translational inhibitor 4E-BP1. Nat. Med. *7*, 1128–1132.

Ulrich-Lai, Y.M., and Herman, J.P. (2009). Neural regulation of endocrine and autonomic stress responses. Nat. Rev. Neurosci. *10*, 397–409.

van Marken Lichtenbelt, W.D., Vanhommerig, J.W., Smulders, N.M., Drossaerts, J.M., Kemerink, G.J., Bouvy, N.D., Schrauwen, P., and Teule, G.J. (2009). Cold-activated brown adipose tissue in healthy men. N. Engl. J. Med. *360*, 1500–1508.

Vegiopoulos, A., Muller-Decker, K., Strzoda, D., Schmitt, I., Chichelnitskiy, E., Ostertag, A., Berriel Diaz, M., Rozman, J., Hrabe de Angelis, M., Nusing, R.M., et al. (2010). Cyclooxygenase-2 controls energy homeostasis in mice by de novo recruitment of brown adipocytes. Science *328*, 1158–1161.

Virtanen, K.A., Lidell, M.E., Orava, J., Heglind, M., Westergren, R., Niemi, T., Taittonen, M., Laine, J., Savisto, N.J., Enerback, S., et al. (2009). Functional brown adipose tissue in healthy adults. N. Engl. J. Med. *360*, 1518–1525.

Watanabe, M., Houten, S.M., Mataki, C., Christoffolete, M.A., Kim, B.W., Sato, H., Messaddeq, N., Harney, J.W., Ezaki, O., Kodama, T., et al. (2006). Bile acids induce energy expenditure by promoting intracellular thyroid hormone activation. Nature *439*, 484–489.

Wijers, S.L., Saris, W.H., and van Marken Lichtenbelt, W.D. (2009). Recent advances in adaptive thermogenesis: potential implications for the treatment of obesity. Obes. Rev. *10*, 218–226.

Xu, B., Goulding, E.H., Zang, K., Cepoi, D., Cone, R.D., Jones, K.R., Tecott, L.H., and Reichardt, L.F. (2003). Brain-derived neurotrophic factor regulates energy balance downstream of melanocortin-4 receptor. Nat. Neurosci. *6*, 736–742.

Xue, B., Rim, J.S., Hogan, J.C., Coulter, A.A., Koza, R.A., and Kozak, L.P. (2007). Genetic variability affects the development of brown adipocytes in white fat but not in interscapular brown fat. J. Lipid Res. *48*, 41–51.

Young, D., Lawlor, P.A., Leone, P., Dragunow, M., and During, M.J. (1999). Environmental enrichment inhibits spontaneous apoptosis, prevents seizures and is neuroprotective. Nat. Med. *5*, 448–453.

Youngstrom, T.G., and Bartness, T.J. (1995). Catecholaminergic innervation of white adipose tissue in Siberian hamsters. Am. J. Physiol. *268*, R744–R751.

Zingaretti, M.C., Crosta, F., Vitali, A., Guerrieri, M., Frontini, A., Cannon, B., Nedergaard, J., and Cinti, S. (2009). The presence of UCP1 demonstrates that metabolically active adipose tissue in the neck of adult humans truly represents brown adipose tissue. FASEB J. *23*, 3113–3120.